Int J Adv Manuf Technol (2017) 91:3121–3134
DOI 10.1007/s00170-016-9935-z

ORIGINAL ARTICLE

A rapid and intelligent approach to design forming shape model for precise manufacturing of flanged part

Chuang Liu[1] · **Hongbing Wu**[1] · **Yimei Yang**[1] · **Junbiao Wang**[1]

Received: 7 June 2016 / Accepted: 18 December 2016 / Published online: 16 January 2017

Abstract Adjusting the part shape with complex flanges to compensate springback deformation is key to forming shape design for manufacturing rapidly and precisely. Classical forming shape design by displacement adjustment (DA) method using finite element (FE) simulation is usually time-consuming and not accurate enough for complex surface part in industrial application. In this paper, the forming shape is modeled by changing the relations of geometric features of part model with the new flange control surfaces directly. Control surface processing (CSP) method is presented including control surface trimming, cross section division, springback compensation, and extending to design forming shape model of doubly curved flange part with joggles rapidly. The algorithms of cross section curves division of control surfaces and subsequent subdivision of each curve with circular arc and line segments are proposed. A case-based reasoning (CBR) technique and gray relation analysis (GRA) are used to support the intelligent springback prediction of each bending segment of the cross section curve. The geometric data of control surface is expressed in XML format to realize the integration of the CAD-based tools of control surface division and compensation with the Web-based springback prediction system. The approach is demonstrated on an industrial aircraft wing rib part. The forming shape model could be designed rapidly by comparison with DA method. The part shape deviations of flange angle (−0.465° ~ 0.528°) and surface position (−0.3 mm ~ 0.3 mm) were detected by comparing the desired geometry with the actual digital formed part shape, and the results indicate that the approach can achieve the industrial part manufacturing rapidly and precisely.

Keywords Design for manufacturing · Control surface processing · Geometric data integration · Forming shape model · Intelligent springback prediction · Precise manufacturing

1 Introduction

Sheet metal-forming processes are extensively used in aircraft industry to produce skin and frame parts. Flanged part with joggles is a major frame type of components in aerospace product, and it is usually jointed with skin in the controlling section of the product body to ensure the product external shape and support aerodynamic load. The web is the main body of the part, and it is flat for most products, the flange is the bent region of the part on the outside of the web, and there are usually flange holes, strengthening socket, strengthening groove, and positioning holes on the web [11]. The flange surface is complex because it is derived from the doubly-curved external aerodynamic shape of the aircraft and the parallel flanges which is connected by joggle to join with other frame parts like a ladder. The part materials are usually aluminum alloys and are formed by rubber hydro-forming machine and tool. Material springback is a phenomenon common to any sheet metal-forming process that leads to the geometric inaccuracy of the resulting shape [12]. Nowadays, the requirements of shape accuracy and manufacturing efficiency are increasing gradually. The springback deformation after forming makes the tool surface different from the part shape and should be compensated [7, 9, 31].

Many researchers are focused on compensating tool surface to form the part rapidly and precisely. Nevertheless, to this kind

✉ Chuang Liu
liuchuang@nwpu.edu.cn

[1] School of Mechanical Engineering, Northwestern Polytechnical University, 127 West Youyi Road, Xi'An 710072, China

of part, the initial tool surface refers to the product external surface and is generally extended by taking die stability, rubber protection, and tool intensity into consideration. Consequently, the objective of springback compensation is to adjust the geometry of product surface to build a new forming shape so that the product will achieve the desired shape after springback [16]. The principle of forming shape design is to measure the shape deviation between the formed part and the desired shape, and compensation would be made in the direction opposite to shape deviation. The process is repeated until the forming shape deviation attains a specified tolerance [7, 9, 31].

The part with complex surface should be divided firstly into simple 2D elements of mesh or cross section curve so that the deformation can be parameterized and predicted exactly to reconstruct the forming shape model. The efficiency and accuracy of forming shape design depend on their representation, prediction and compensation of springback errors, the data integration of different computer-aided systems, and subsequent three-dimensional (3D) modeling.

Simulation-based evaluation and verification of design solutions reduce trial-and-error experiments in workshop, shortens product development lead-time, and improves product quality and productivity [6]. Finite element (FE) simulation is widely used to predict springback errors, where flange surface is divided into meshes. The errors are represented by the linear displacement of each node from its initial position to a new position after springback. Typical compensation method is displacement adjustment (DA) method [7]. For the each cycle of compensation, the linear displacement adjustment of each node could be performed by its desired position and formed point after springback along the *y*-axis vector along one point [7], straightforward vector connecting two points [14], normal vector of the new point on the springback contour curve [3], or the initial point on the desired contour curve [30]. As the springback compensation for an industrial product by DA methods using FEA can be very time-consuming and cost-intensive, the demand for a compensating algorithm is high [15]. It takes 3 cycles for the DA method to reach the forming accuracy for a U cross section part [7]. The current research results indicate that there are errors between the results of FE simulation and practical formation [15]. Compensation factor is used to adjust the theoretically compensated geometry to decrease the number of cycles [16, 30]. For example, the improved sheet elements compensation (SEC) method still needs three iterations for continuous doubly curved bending shape less than 100 mm long [31]. As a result, and despite significant research efforts to date, the application of FE analysis to predict shape geometric deviations caused by springback is still very limited [12]. To complex surface with abrupt changes, the surface compensation process is also challenging. The surface-controlled overbending (SCO) method was presented to optimize the tool shape of a deep drawing product by constructing a simplified reference surface and compensated transformation surface [14]. How to create control surface and avoid surface transforming to build the forming shape rapidly should be further studied.

The part surface can be also divided into cross section curves of the flange by normal plane of discrete points along the flange boundary line. The springback can be represented by angular displacement, and the arc radius and angle after springback can be calculated rapidly by using an analytical method, such as for the U-section part [10, 18] or arcs of an arbitrary channel [2], or knowledge-based method, such as neural network [9, 19], or three-dimensional scanning data comparison method [28]. As some practical process conditions cannot be taken into account, there are usually some deviations between the predicted value and practical one by analytical calculation [2]. In terms of empirical practices, some guidelines and past experience utilization have been proposed aiming to increase the geometric accuracy [12, 20]. Knowledge-based springback prediction method might become more reliable to allow industrial application if there is enough empiric knowledge. To meet the demands of rapid responsibility and high flexibility, effective reuse of enterprise knowledge is a key strategic component of product development [22]. In some manufacturing activities, such as process planning [26] and manufacturability analysis [4], knowledge retrieval is performed based on similarity of product or process. Case-based reasoning (CBR) is regarded as a potential method, since it is similar to human being's reasoning process [21], and it is a chief reference tool in engineering design [8]. Designer can determine the parameter values of new product through analogical reasoning on these similar retained cases [5]. The case is represented as feature vector that includes problem features and corresponding solution. A good assessing similarity between cases is a key success of CBR [25]. Multiple similarity measure metrics have been used such as ratio function, Euclidian distance function, Manhattan distance function, and so on [21]. The one which shows the similarity directly can be selected to assess the similarity of current part and retained cases [8, 27]. For example, correlative value in gray relation analysis (GRA) can be used [21].

Integration of design model with process information in real-time is necessary in order to increase product quality and shorten the product manufacturing cycle [24]. To bridge the gaps between CAD and CAE tools, geometric model in a CAD tool is transferred to a CAE tool via the third-party interfaces, e.g., STEP, IGES, and STL for FE analysis [17], and the adjusted forming shape surface of mesh data in a CAE tool must be reconstructed in CAD system, but the subdivision model needs to be converted to NURBS to interact with the rest of the CAD system [1], such as to be used in tool model design. This is also time-consuming to meet the precision of being suitable in the manufacturing phases of design. Knowledge-based springback prediction is more efficient than FE simulation, but it needs parameterized and exchangeable

representation of the 2D cross section curve. In order to simplify the description and operation of digital curves, the curve is approximated by suitable primitives such as circular arcs and line segments [13], and heuristic algorithm can be used to divide the curve into segments [23]. The product model is developed using XML-based representation for product data required for process planning [22, 24], and this is a very useful approach for direct distributed applications [24], such as automating design calculations and CAD drawings [29]. So, it is possible to develop XML-based surface division data expression to integrate the CAD with web-based software for building the compensated surface more efficiently.

The goal of this research is to present an industrially applicable approach to design forming shape model of the complex flanged part for precise manufacturing. A series of control surface processing (CSP) algorithms are proposed to design the control surface of the 3D forming shape model rapidly and precisely, and XML-based integration of CAD system and web-based system is developed to realize the CBR-based prediction of the springback errors intelligently and control surface compensation. How the compensated result is used to design the forming shape model and manufacture the part is demonstrated on an industrial aircraft wing rib part. A manufacturing test is carried out to verify its validity.

2 Design process from product model to forming shape model

Figure 1 shows the five main models of the part with complex flanges in its precise manufacturing process. 3D part model defines the geometry, dimension, tolerance, and technical notes. Forming shape model is a temporary state when the force is still imposed in the forming process. It is designed for manufacturing precisely by compensating for unintentional but unavoidable processing deformation. The die model is then built by extending forming shape and used to fabricate the tool. After the aluminum alloy part is formed in new quenching state and pressure is unloaded, the flange will spring back to desired shape and the physical properties are achieved. The practical part geometry is digitalized by means of a 3D optical scanning system. Then, the measured point cloud model is acquired and compared with the desired part surface to create the data analysis model to show the forming deviation.

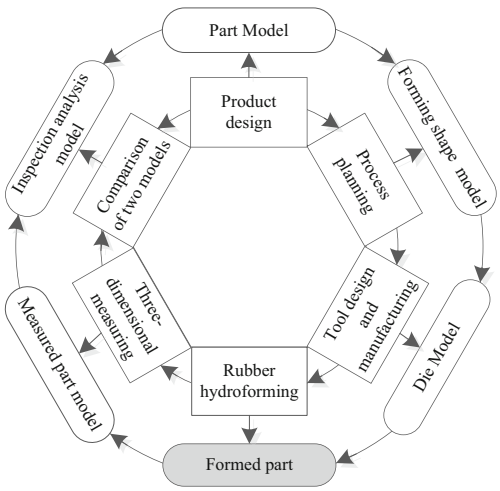

Fig. 1 Data models in the precise manufacturing cycle

2.1 Part model design process

3D part model is composed of geometrical, annotation, and notes sets. Geometrical set contains part body, external references, and construction geometry. Annotation set contains view, datum, geometrical dimension, and tolerance. Notes set contains standard notes, part notes, material description, etc. Part body defines the part shape and dimension that is built from a series of features. External references, such as stringer axis line, frame datum plane, theoretical external aircraft surface, and so on, are referred to by the part body and they are the interfaces that determine the father-son relationship between the part model and the aircraft product master geometrical model. Construction geometry contains the intermediate geometric elements such as points, lines, and planes to aid the part body modeling, which should be properly named, organized, associated, and retained for consequent change and utilization.

As shown in Fig. 2, the relations of the geometrical elements are illustrated by a wing rib part model built by mechanical design in CATIA system. The part control surface is created in construction geometry by offsetting the theoretical

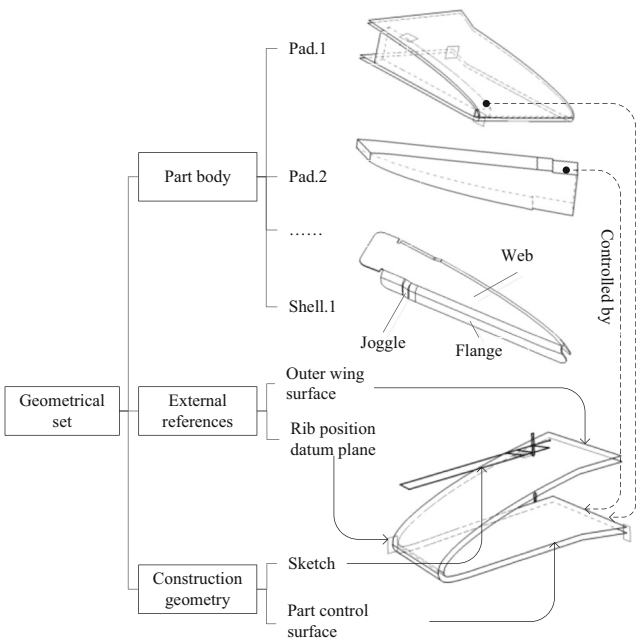

Fig. 2 The geometrical set and relations among them of 3D part model

external wing surface inward the thickness of the skin. The web and sketch plane is determined by the rib position plane, and the sketch drawing is drafted. The initial part body is created by the sketch drawing and stretching direction and control surface. The joggled flanges, which refer to the part control surface or the joint part surface, should be designed to sidestep the joint stringers which are vertical to the part. In this case, the joggled flange is controlled by the partial part control surface. The parallel joggled flanges may be created by several methods. For example, the sketch drawing is drafted on the edge of joint part, the body is created, and subtraction operation is performed in the main part body. The joggles are created by chamfer modeling, and the stringer notch, stiffening socket, stiffening slot, and lightening hole are modeled by the standard sizes if necessary. So, the relations of the control surface and the part body are built by feature modeling. The flange surfaces are trimmed, and intersections are rounded to form the final part surface. The final part model is created by shell feature modeling.

2.2 Forming shape model design process

The forming shape is designed by adjusting the product model according to the springback errors, and it decides whether the part is formed precisely or not. How to design the forming shape is decided by the complexity of the part surface. As shown in Fig. 3, the case part has two side flanges and two joggles. The radius of curvature in curvature boundary line and each cross section curve is variable, and the flange height and bending angle are also variable. For the flange and cross section curve shown in Fig. 3a, the radius of curvature in the boundary line is from 14.515 to 1466.529 mm, and that in cross section curve is from 187.976 to 308.601 mm separately. The bending angle is from 68.505° to 84.601°. The joggle features make the flange surface change abruptly like a ladder. There are many small irregular curved surfaces because of joggles or stringer gaps on the flange and filets on the intersections. If these small surfaces are compensated independently, the design process is tedious and the accuracy is difficult to ensure. Consequently, it is difficult to build the forming shape surface if the part surface is adjusted directly.

As shown in Fig. 4, this paper presents a new forming shape model design approach that includes control surface processing (CSP), intelligent prediction of springback angle, and forming shape modeling. CSP operations consist of part control surface trimming, division, compensation, and extending to create the forming shape control surface. The presented algorithms are used to develop three specific software tools: CAD-based control surface division tool, CAD-based control surface compensation tool, and web-based intelligent springback prediction system to realize the integrated forming shape model design rapidly and precisely. They all have integration interfaces in which the control surface division data is expressed as XML format.

Step 1: Trim the exterior part control surfaces into separate flange control surfaces S_i^C by the part profile and flanges relations and further create arc surfaces S_i^{CA} and flange surfaces S_i^{CF} ($i = 1, 2, \cdots, G$), where G is the number of the flanges. If the flanges on one side are controlled by the same surface, that control surface should be trimmed only one time.

Step 2: Divide each flange control surface into cross section curves set of bending arc section L_{ik}^A and flange section L_{ik}^F ($k = 1, 2, \cdots, Q_i$), approximate the flange section L_{ik}^F with the circular arcs and straight line segments $Seg_{it}(t = 1, 2, \ldots\ldots, T_i)$, and store the division data in XML format for springback prediction.

Step 3: Predict each cross section curve's springback error based on knowledge base, add the compensated angle and radius to each cross section curve's data, and output it to the XML file for control surface compensation.

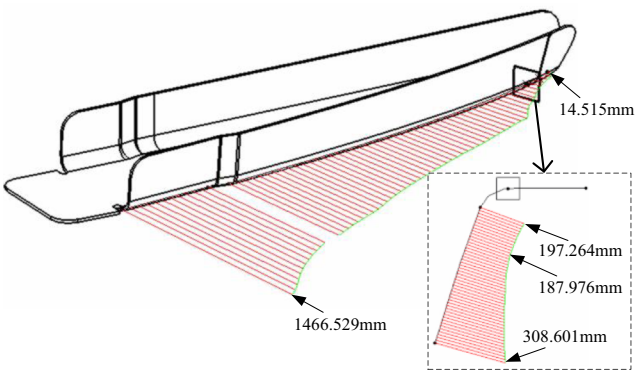

(a) The case part

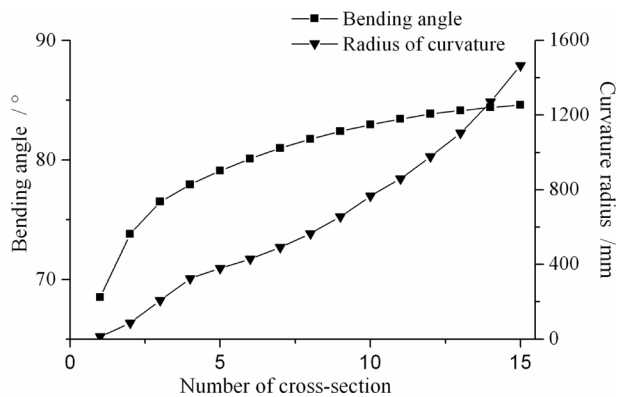

(b) Bending angle and radius of curvature of one side flange

Fig. 3 The one-side flange surface analysis data of the case part. **a** The case part and **b** bending angle and radius of curvature of one side flange

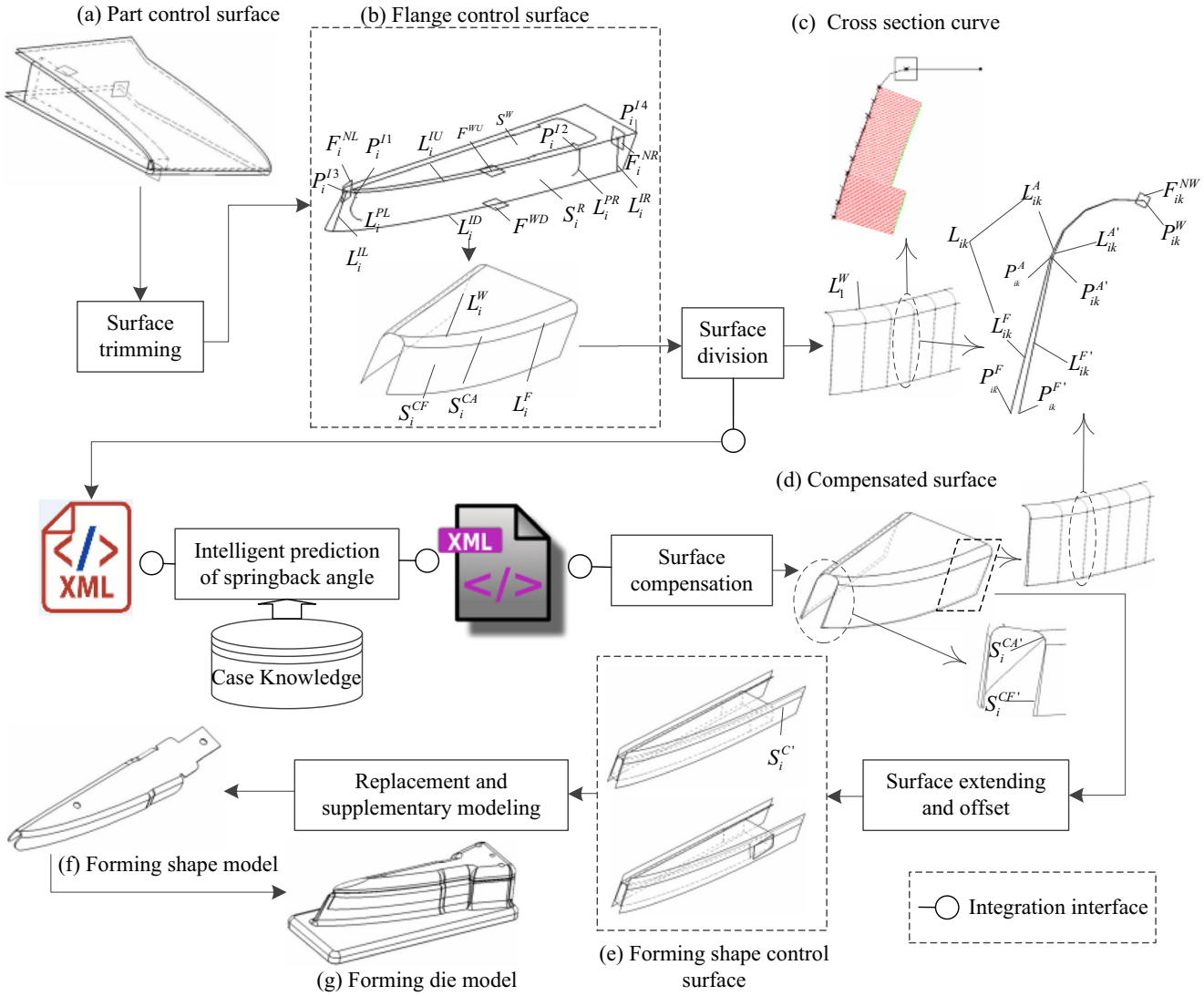

Fig. 4 Forming shape model design process

Step 4: Compensate cross section curves after parsing XML-based cross section segments set data and reconstruct them to create the forming shape control surfaces $S_i^{CA'}$ and $S_i^{CF'}$.

Step 5: Extend, trim, and translate the forming shape control surfaces to create the new flange control surfaces $S_i^{C'}$ of the forming shape model.

Step 6: Replace the original flange control surfaces S_i^{C} with the corresponding new surfaces $S_i^{C'}$ by the relations of the part body feature and construction geometry to change the part model into the forming shape model. Positioning holes and ears features are added to the model.

This approach is different from the surface controlled overbending (SCO) method [15]. To surface adjustment, without complicated construction of reference and transformation surfaces in SCO, CSP uses the part control surface directly and the compensated surfaces are directly used for forming shape modeling. To springback compensation of the surface, this approach uses cross section division, not mesh division, and knowledge-based reasoning, not FE simulation for each discrete element. To forming shape modeling, not the relations between reference surface and original surface but the relations of geometric elements are reused to build the forming shape more rapidly.

3 Control surface processing method

3.1 Trimming of part control surfaces

Trimming of part control surfaces is shown in Fig. 4b. The control surface S_i^C ($i=1,2,\cdots,G$) of each flange is created

by copying the original control surface and firstly trimmed by the intersection line L_i^{IU} and L_i^{ID} to keep the intermediate surface. The plane F^{WU} which the external surface S^W of the web belongs to is intersected with the flange control surface S_i^C to create the intersection line L_i^{IU}. The plane F^{WD} is created by translating the plane F^{WU} h down along its normal direction, where h is about maximum of flange height added 10 mm, and intersects with the surface S_i^C to create the intersection line L_i^{ID}.

The control surface S_i^C is further trimmed by L_i^{IL} and L_i^{IR} to keep the intermediate surface. The two circumferential boundary lines of the flange which refers to the surface S_i^C are projected onto S_i^C to create the line L_i^{PL} and L_i^{PR}. The two lines intersect with L_i^{IU} to create two points P_i^{I1} and P_i^{I2}. These two points are extended outward to P_i^{O3} and P_i^{O4} of L_i^{IU} separately until the lines of L_i^{PL} and L_i^{PR} is between the normal planes F_i^{NL} and F_i^{NR} on these two points. The plane F_i^{NL} and F_i^{NR} intersects with the surface S_i^C on the line L_i^{IL} and L_i^{IR} separately.

The plane F^{WU} is trimmed by the surface S_i^C, F_i^{NL}, and F_i^{NR} to create the extended web plane S_i^W. On the intersection line L_i^{IU} of the extended web plane S_i^W and the flange control surface S_i^C, the chamfer is created by the radius of the bent region of external flange surface to create the arc surfaces S_i^{CA}. The boundary line L_i^W of arc surface adjacent to web is the intersection line of S_i^{CA} and S_i^W, and it further trims the plane S_i^W. The boundary line L_i^F of arc surface adjacent to flange surface is the intersection line of surface S_i^{CA} and S_i^{CF}, and it trims the surface S_i^C to create the flange surface S_i^{CF}. The surface of S_i^{CA} and S_i^{CF} together groups flange control surfaces which is used to design the forming shape control surface.

3.2 Division of the flange control surface

As shown in Fig. 4b, to the ith flange control surface that is composed of the bending arc section S_i^{CA} and flange section S_i^{CF} ($i=1,2,\cdots,G$), its division algorithm (Fig. 5) includes the division of surface into cross section curves, the subdivision of flange section curve into points and its approximation with circular arc and straight line segments (Fig. 4c).

Step 1: Divide the arc surface boundary line L_i^W into equidistant points at interval d_i^W into P_{ik}^W ($k=1,2,\cdots,Q_i$), where $d_i^W = 1\sim 2mm$, $Q_i = \left\lceil \frac{l_i^W}{d_i^W} \right\rceil + 1$, l_i^W is the length of L_i^W.

Step 2: Create normal planes F_{ik}^{NW} of P_{ik}^W on L_i^W, intersection line L_{ik}^A of F_{ik}^{NW} and S_i^{RA}, and intersection line L_{ik}^F of F_{ik}^{NW} and S_i^{RF}, and group L_{ik}^A and L_{ik}^F into cross section curve L_{ik} (that is flange element), where L_{ik}^A is bending arc section $P_{ik}^W P_{ik}^A$ with arc radius R_{ik}^A and central angle θ_{ik}^A, L_{ik}^F is flange section of arbitrary curve $P_{ik}^A P_{ik}^F$, and the tangent vectors of P_{ik}^W, P_{ik}^A and P_{ik}^F on L_{ik} are $\overrightarrow{V_{ik}^{TW}}$, $\overrightarrow{V_{ik}^{TA}}$ and $\overrightarrow{V_{ik}^{TF}}$ separately.

Step 3: Approximate L_{ik}^F with circular arc and straight line segments which can be represented by primitive geometric element of points, length, radius, and center point.

Step (a): Divide L_{ik}^F into equidistant points $P_j(x_j,y_j,z_j)$ ($j=1,2,\cdots,N_{ik}$) at interval d, where $d=1\sim 3mm$, $N_{ik}=\lceil l/d \rceil+1$, the curvature of $P_j(x_j,y_j,z_j)$ is K_j, the tangent vector of $P_j(x_j,y_j,z_j)$ is $\overrightarrow{V_j}$. The intermediate point is to be deleted if $K_j=K_{j+1}=K_{j+2}$ ($j=1,2,\cdots,N_{ik}-2$), and the surplus points are renumbered as $P_j\left(x_j,y_j,z_j\right)\ \left(j=1,\cdots,N_{ik}^{'}\right)$, where $N_{ik}^{'}$ is the number of points after merging. Let $L=N_{ik}^{'}$.

Step (b): If K_j and K_L is 0, then the two adjacent points determine a straight line segment; otherwise, $P_j,\cdots\cdots,P_L$ are approximated as a circular arc. If the approximating error $\overline{P_{j,L}}$ is less than given division deviation, then a new circular arc segment is created. Otherwise, set $L=L-1$. This step is repeated until the points can be approximated as a circular arc within the tolerance.

The approximating error of the circular arc can be evaluated by

$$\overline{P_{j,L}} = \sum_{u=j}^{L} \left| R - \left| \overrightarrow{P_u O} \right| \right| \Big/ (L-j+1), \tag{1}$$

where R and O are the radius and centre point of the circular arc respectively.

The radius is calculated by

$$R = \left| \overrightarrow{P_j P_L} \right| \Big/ \sqrt{2\times(1-\cos\theta)}, \tag{2}$$

where θ is the central angle of the circular arc.

The central angle is calculated by

$$\theta = \arccos\left(\left(\overrightarrow{V_j} \cdot \overrightarrow{V_L} \right) \Big/ \left(\left| \overrightarrow{V_j} \right| \left| \overrightarrow{V_L} \right| \right) \right). \tag{3}$$

Step (a): Let $j=L$ and $L=N_{ik}^{'}$, the step (b) is repeated until all the points are approximated as circular arc or straight line segments.

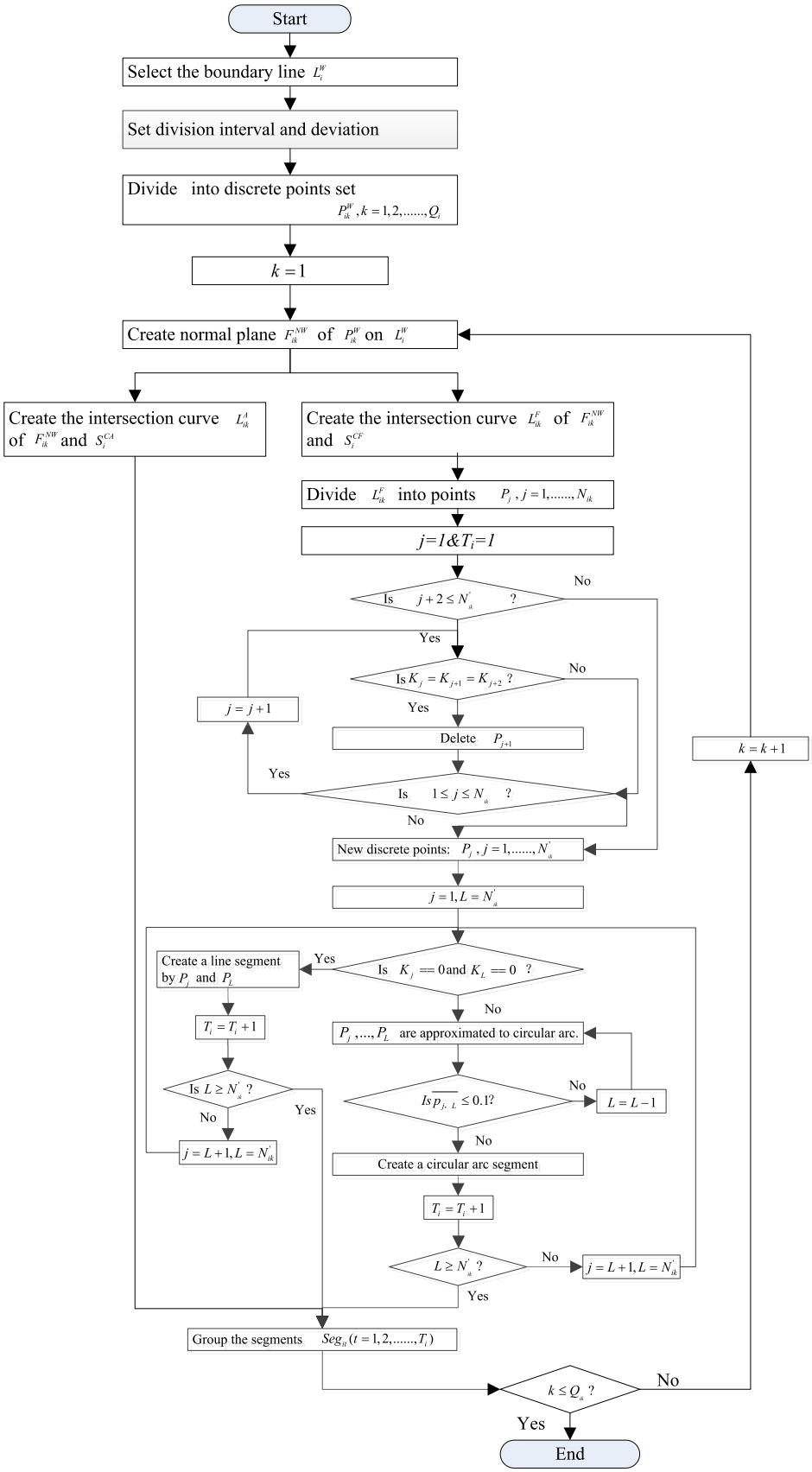

Fig. 5 Division of the flange control surface

Step (b): Group the segments $Seg_{it}(t=1,2,.....,T_i)$ to approximate the flange section curve L_{ik}^{F} where the joint point of two adjacent equal curvature segments should be first-order continuous.

As shown in Fig. 6, the flange control surface division software tools were developed based on the CATIA V5 R18 using Component Application Architecture (CAA), and it provides the output interface of XML-based surface division data. The surface after division is decomposed into parameterized circular arc and straight line segments, and expressed in the XML file to integrate with the knowledge-based system. The radius of and central angle is 0 if the segment is straight line. Each piece of data is enclosed in the defined markup tags, which are arranged in a hierarchy that represents the ordering of the data in a parent/child relationship.

The cross section curve of the flange element shown in Fig. 3a is divided into ten points; the coordinates and curvatures of the points are shown in Table 1. The former six points are approximated by one arc segment with radius 202.724 mm and arc angle 3.488°, and the maximum deviation of the points to the arc is 0.014 mm. The next four points are approximated by the other arc segment with radius 273.81237 mm and arc angle 1.291°, and the maximum deviation of the points to the arc is 0.018 mm. The part with flanges forming deviation is usually below 0.5 mm, and the forming die fabricating deviation is usually below 0.1 mm, so the distance between the reconstructed surface and original surface is set less than 0.1 mm. The deviations are less than 0.1 mm, so the cross section curve approximation is acceptable.

To judge whether the surface division is acceptable or not, a new surface is reconstructed by the cross section curves and compared with the original part geometry. The maximum distance between the two surfaces is selected as the judging index. The length of the flange in Fig. 3a is 173.789 mm, and the bending angle varies from 68.506° to 84.601°. The surface is divided at intervals 1, 1.5, 2, 2.5, and 3 mm, the cross section curve is divided at interval 0.1 mm. The deviations are all less 0.02 mm, so the division interval 1 ~ 3 mm can meet the shape tolerance of surface division and reconstruction.

3.3 Compensation of the flange control surface

As shown in Fig. 7a, after the division of the flange control surface S_i^{CA} and $S_i^{CF}(i=1,2,.....,G)$, the springback errors

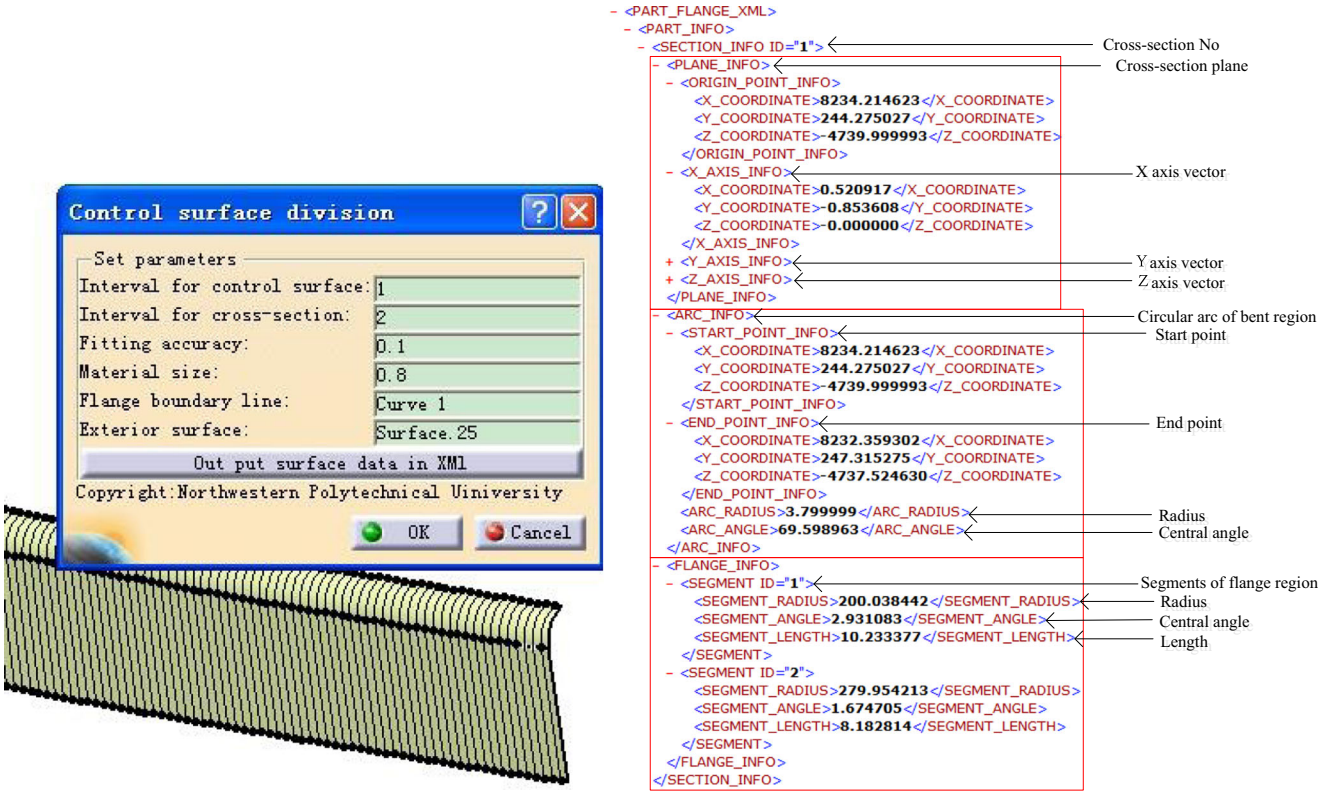

Fig. 6 Flange control surface division tool and data expression. **a** Flange control surface division tool and **b** XML-based Flange control surface division result

Table 1 The coordinate, radius, and deviation of the example partition points (/mm)

No.	Coordinate	Radius	Deviation
1.	(8231.457, 246.735, −4737.562)	197.264	0
2.	(8231.065, 247.348, −4735.63726)	188.861	0
3.	(8230.6854, 247.94291, −4733.706)	188.204	0.002
4.	(8230.317, 248.520, −4731.768)	193.941	0.006
5.	(8229.959, 249.080, −4729.822)	208.312	0.010
6.	(8229.612, 249.624, −4727.867)	226.390	0.014
7.	(8229.266, 250.165, −4725.913)	245.740	0.015
8.	(8228.945, 250.668, −4723.943)	265.463	0.016
9.	(8228.624, 251.170, −4721.973)	284.198	0.017
10.	(8228.302, 251.675, −4720.005)	308.60	0.018

should be compensated for each cross section curve. The springback errors of the cross section curves are predicted by knowledge-based reasoning (Sect. 0). The curvatures of the surface S_i^{CF} are usually very small (0.000129~0.005361 mm^{-1} in the part shown in Fig. 3), so its springback can be ignored. After the springback prediction result stored in XML file is read, each cross section curve of the bending circular arc segment L_{ik}^{A} $(k=1,2,\cdots,Q_i)$ is adjusted using the compensated radius $R_{ik}^{A'}$ and central angle $\theta_{ik}^{A'}$ to make the flange element achieve the desired shape after springback. The segments of the flange section L_{ik}^{F} are adjusted with the change of the adjacent circular arc L_{ik}^{A}. The flange control surface compensation tool was developed based on the CATIA V5 R18 using CAA, and it provides the input interface of XML-based surface division data with springback parameters (Fig. 7b).

The compensated arc segment $L_{ik}^{A'}$ is created with start point P_{ik}^{W}, tangent vector $\overrightarrow{V_{ik}^{TW}}$, radius $R_{ik}^{A'}$, central angle $\theta_{ik}^{A'}$, and endpoint $P_{ik}^{A'}$ by the principle that the neutral layer length is not changed before and after springback. After that, the first segment Seg_{i1} in L_{ik}^{F} is translated along $\overrightarrow{P_{ik}^{A}P_{ik}^{A'}}$ by $\left|\overrightarrow{P_{ik}^{A}P_{ik}^{A'}}\right|$ in normal plane F_{ik}^{NW} and rotated around normal vector $\overrightarrow{V_{ik}^{N}}$ of $P_{ik}^{A'}$ on F_{ik}^{NW} to make $L_{ik}^{A'}$ and the adjusted segment $Seg_{i1}^{'}$ tangent-continuous at $P_{ik}^{A'}$. The other segments are adjusted one by one by keeping tangent-continuous with the former segment and constant in radius and angle or length, and the new segments $Seg_{it}^{'}(t=1,2,.....,T_i)$ group the compensated flange section curve $L_{ik}^{F'}$. The cross section curves of $L_{ik}^{A'}$ and $L_{ik}^{F'}(k=1,2,\cdots,Q_i)$ are used to reconstruct the new flange control surface of $S_i^{CA'}$ and $S_i^{CF'}$ $(i=1,2,.....,G)$ (Fig. 4d) using multi-section surface modeling in CAD system.

4 Intelligent prediction of springback angle

The central angle of $L_{ik}^{A'}$ in Fig. 7a is computed by

$$\theta_{ik}^{A'}=\theta_{ik}^{A}+\Phi_{ik}, \tag{4}$$

where θ_{ik}^{A} is the original central angle of L_{ik}^{A}, $\theta_{ik}^{A'}$ is the central angle after springback compensation, and Φ_{ik} is the predicted springback angle.

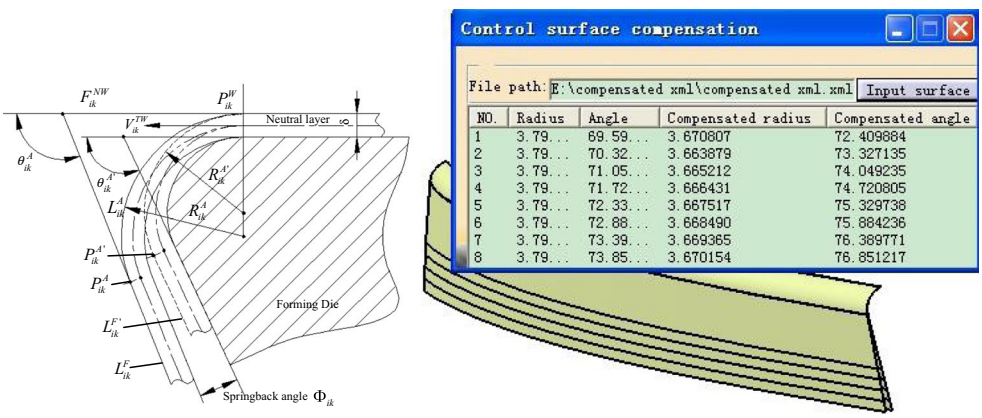

(a) Principle of springback compensation (b) Flange control surface compensation tool

Fig. 7 Flange control surface compensation principle and the software tool. **a** Principle of springback compensation and **b** flange control surface compensation tool

The radius of $L_{ik}^{A'}$ is computed by

$$R_{ik}^{A'} = \frac{\theta_{ik}^{A}}{\theta_{ik}^{A} + \Phi_{ik}} R_{ik}^{A} - \frac{\Phi_{ik}}{\theta_{ik}^{A} + \Phi_{ik}}(1-K)\delta, \quad (5)$$

where R_{ik}^{A} is the original radius of L_{ik}^{A}, K is neutral layer factor of the sheet acquired from the manual, and δ is the material thickness.

The springback angle Φ_{ik} of bending circular arc L_{ik}^{A} is predicted by case-based reasoning (CBR) method. To the part with same material type, the springback angle is attained by retrieving the case from the knowledge base which is most similar to the current geometric feature of bending circular arc segment. Gray Relation Analysis (GRA)-based similarity measuring method is adopted to compute the gray relational degree as measures of similarity. GRA is capable of solving the complicated interrelationships among designated feature values [21, 27]. The gray relational degrees of the cases to the current problem are computed as follows:

Firstly, the feature data sequence is set up by the current arc section and m similar cases as $CA = \{C_u/u = 0, 1, 2, \cdots, m\}$, where $C_u = (x_{u1}, x_{u2}, \ldots, x_{uv}, \ldots, x_{un}), v = 1, 2, \cdots \cdots, n$, x_{uv} represents the vth problem feature component of the uth case.

The springback angle prediction case of the bending circular arc segment is represented as follows: problem feature = (x_1, x_2, x_3) = (material thickness, bending radius, bending angle), solution feature = (springback angle). The part material is 2024-O aluminum alloy, and the thickness is 0.8 mm. The part is formed when the material is in the W state. Table 2 shows the cross section flange element in the Fig. 3a and its similar cases.

Before the relational analysis, the feature data from similar case set are converted into the dimensionless data to avoid the different dimensions and magnitudes, and the linear normalization is expressed as follows:

$$x_{uv} \rightarrow f(x_{uv}), f(x_{uv}) = x_{uv}/x_{0v}, u \in M = \{0, 1, 2, \cdots, m\}, v \in N = \{0, 1, 2, \cdots, n\} \quad (6)$$

Table 2 Feature data sequence of the case cross section

No	x_1/mm	x_2/mm	x_3/°	Springback angle/°
C0	0.8	3.0	74.597	
C1	0.64	2.38	75	2.5
C2	0.64	2.38	70	2.25
C3	0.64	3.18	75	3.75
C4	0.64	3.18	70	3.5
C5	0.81	2.38	75	2
C6	0.81	2.38	70	2
C7	0.81	3.18	75	3.25
C8	0.81	3.18	70	3

Table 3 Feature data conversion of the case cross section

No.	f_1	f_2	f_3
C0	1	1	1
C1	0.8	0.793333	1.0054
C2	0.8	0.793333	0.9384
C3	0.8	1.06	1.0054
C4	0.8	1.06	0.9384
C5	1.0125	0.793333	1.0054
C6	1.0125	0.793333	0.9384
C7	1.0125	1.06	1.0054
C8	1.0125	1.06	0.9384

Table 3 shows the dimensionless data converted from the feature data sequence of Table 2.

After that, the gray relational coefficient between f_{uv} and f_{0v} of vth feature component of C_u and C_0 is expressed as follows:

$$\zeta_{0u}(v) = \frac{\min\limits_{u \in M} \min\limits_{v \in N} s_u(v) + \rho \max\limits_{u \in M} \max\limits_{v \in N} s_u(v)}{s_u(v) + \rho \max\limits_{u \in M} \max\limits_{v \in N} s_u(v)}, \quad (7)$$

where $s_u(v) = |f_{0v} - f_{uv}|$ and ρ ($\rho \in [0, 1]$) is a distinguishing parameter to show the relational degree between f_{uv} and f_{0v}, and is set as 0.5 in this paper.

The relational degree of C_u and C_0 is expressed as follows:

$$\gamma(C_0, C_u) = \sum_{v=1}^{n} \omega_v \zeta_{0u}(v), \quad (8)$$

where $\gamma(C_0, C_u) \in (0, 1]$ and ω_v is the weight of every feature component that meets $\sum_{i=1}^{n} \omega_i = 1$.

The greater $\gamma(C_0, C_u)$ is, the closer it is to C_0. The cases of which the similarity is more than the threshold value are ranked by its relational degree, and the most similar one is reused to get its solution feature as the predicted springback angle.

The weights of material thickness, bending radius, and bending angle are determined by data analysis of orthogonal experiment using FEA with $\omega_1 = 0.43$, $\omega_2 = 0.37$, and $\omega_3 = 0.2$. The calculation result is shown in Table 4, and the similarity is

Table 4 The similarity of the case to current cross section

No.	$\zeta_{0u}(1)$	$\zeta_{0u}(2)$	$\zeta_{0u}(3)$	$\gamma(C_0, C_u)$
C1	0.3585	0.3508	1.0000	0.4839
C2	0.3585	0.3508	0.6592	0.4158
C3	0.3585	0.6657	1.0000	0.6005
C4	0.3585	0.6657	0.6592	0.5323
C5	0.9387	0.3508	1.0000	0.7334
C6	0.9387	0.3508	0.6592	0.6653
C7	0.9387	0.6657	1.0000	0.8500
C8	0.9387	0.6657	0.6592	0.7818

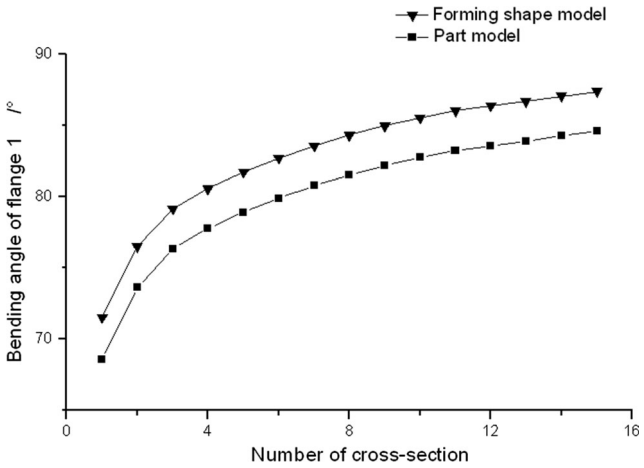

Fig. 8 Bending angle of the part and forming shape model

between 0.4158 and 0.8500. The threshold value is 0.75, so C7 or C8 may be reused. To this case, the most similar case C7 is reused and the predicted springback angle is 3.25°.

Figure 8 shows the original and compensated bending angle of one side flange of the part model in Fig. 3a. The springback angle varies from 2.75° to 3.25° corresponding to the change for bending angle from 68.505° to 84.601°. To the cross section element of the same material thickness, the springback angle increases with the bending angle.

As shown in Fig. 9, the knowledge-based springback prediction system including the integration interfaces with the control surface division and compensation tools was developed based on B/S architecture using J2EE. After reading the flange control surface data expressed in XML file from CAD system, the springback angle and radius are computed and used to compensate the bending arc section. The result is stored and added to the interface XML file for surface compensation in CAD system.

5 Forming shape modeling by relational design

This paper facilitates the forming shape model design by changing the features of the 3D part model. As mentioned in 2.1, the part body is related to its flange control surfaces, and when these surfaces are replaced by the new forming control surfaces, the related flange surface of the part body will change as well. The forming shape control surfaces $S_i^{C'}$ are created by extending $S_i^{CF'}$ upward $2R_i^{A'}$ by keeping continuous in curvature and used to replace the original flange control surfaces S_i^C $(i=1,2,\cdots,G)$, where $R_i^{A'}$ is the average compensated radius of S_i^C and computed as follows

$$R_i^{A'} = \frac{1}{Q_i}\sum_{k=1}^{Q_i} R_{ik}^{A'}(k=1,2,\cdots,Q_i). \tag{9}$$

As shown in Fig. 10, the part model is changed and the forming shape model is then built rapidly. The ears and positioning holes are created to achieve the final forming shape model.

6 Industrial application of forming shape model

Figure 11 shows the application of the forming shape model of the case part into its manufacturing. By DA method using FE simulation, it took about 30 min to simulate the forming process, 5 min to simulate the part's springback, and 60 min to adjust the forming shape surface with workstation computer with CPU of Intel Xeon E5–1603 V3 and internal memory of 4G for the case part. If the desired shape is achieved after three iterations that is the average cycles in the literature, the part forming shape surface compensation takes at least 285 min. It

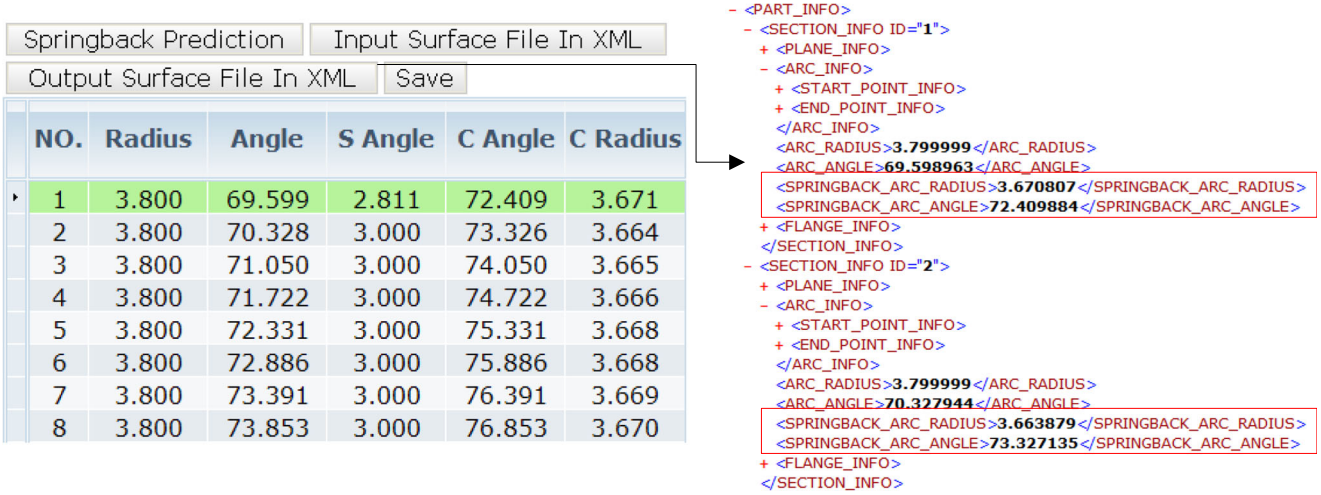

Fig. 9 Knowledge-based springback prediction system

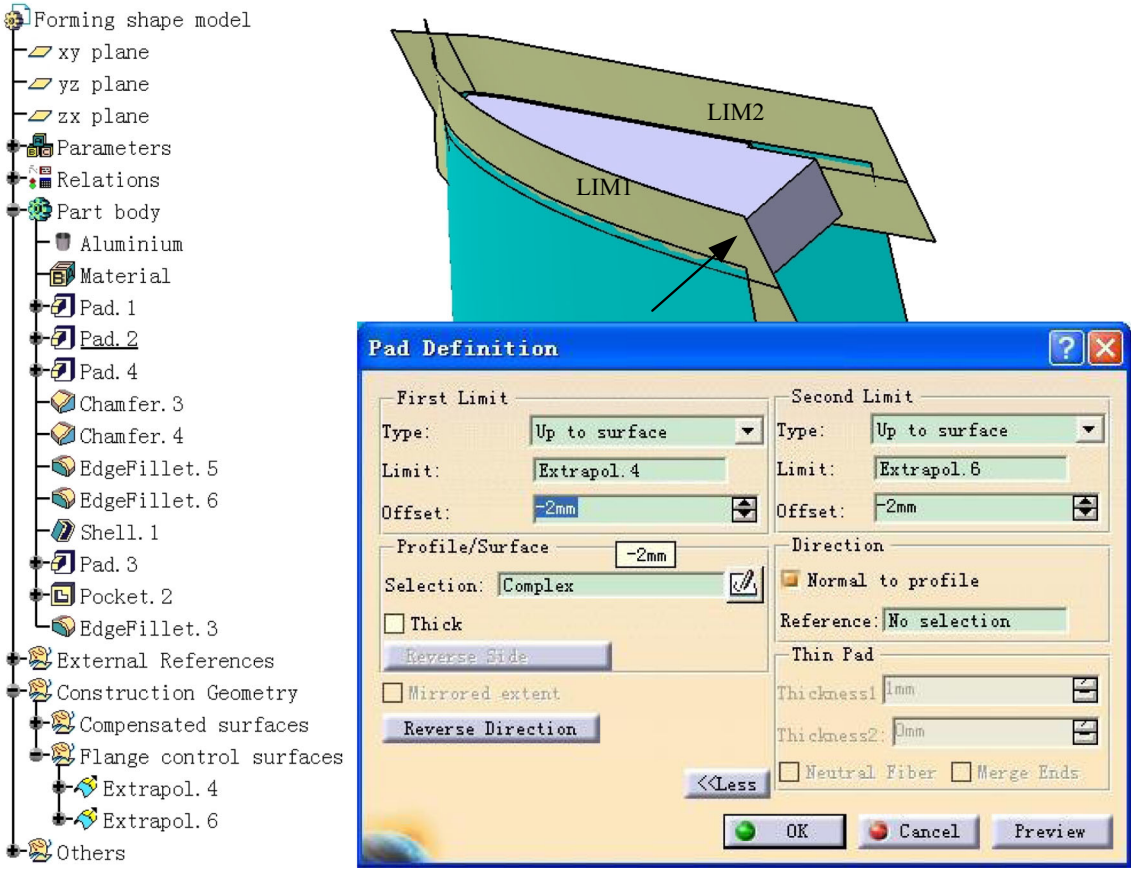

Fig. 10 Forming shape control surfaces replacement

took about 35 min to design the 3D forming shape model, including 20 min to trim and divide the surfaces by the flange surface division tool, 10 min to predict the springback by the knowledge-based prediction system, and 5 min to construct the forming shape control surface by the control surface compensation tool. The forming shape design cycle is reduced obviously by the proposed method and tools.

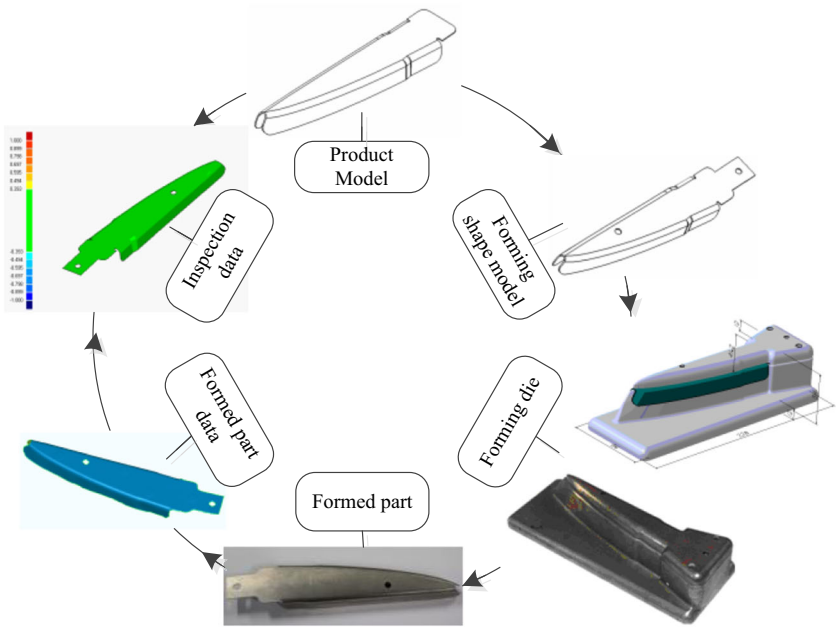

Fig. 11 Manufacturing process of the case part

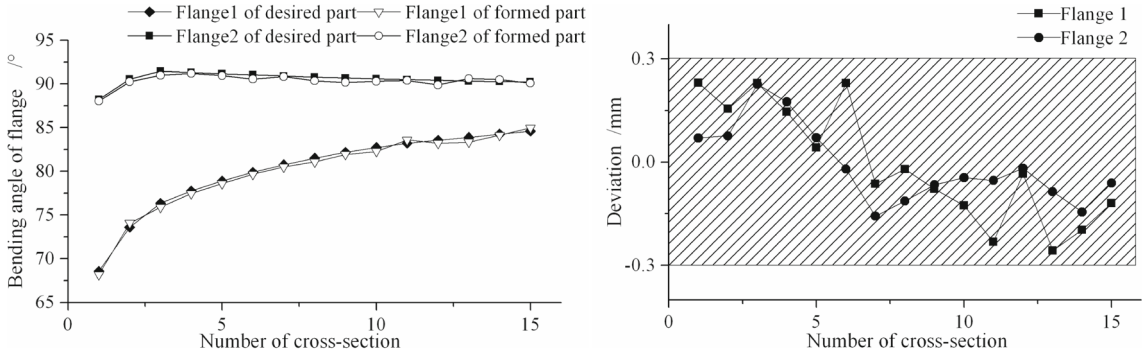

(a) Flange angle deviation (b) Outer shape position deviation

Fig. 12 Manufacturing deviations of the case part. **a** Flange angle deviation. **b** Outer shape position deviation

The inner surface of the forming shape model is used to design the tool surface. Because the narrow end makes the tool unstable, the stiffened structure is added to the tool surface. The die was fabricated by NC machine and the part was formed in new quenching state by rubber hydroforming machine with pressure = 250 bar. The practical part geometry digitalized by means of a 3D optical scanning system was compared with the desired part surface, and the deviation was analyzed as shown in Fig. 12. The position tolerance of the part flange is between −0.5 and +0.5 mm, and the angle tolerance is between −1° and +1°. Figure 12a shows that the angle deviation is in the range of −0.465°~0.528° and the average value is 0.207°. The springback rate of this part is about 3.89%. Figure 12b shows that the position deviation is in the range of −0.3~0.3 mm, and the average value is 0.118 mm. So, the part was manufactured precisely by the forming shape tool.

7 Conclusion

In this research, our main contribution is the approach to design forming shape model of the flanged part with joggles for manufacturing. The tests and analysis results reveal that this approach makes it possible to manufacture an industrial part rapidly and accurately.

1. To doubly-curved flange with joggles, the proposed control surface processing (CSP) method mainly includes control surfaces trimming, division, and compensation. It adjusts not the whole part surface directly, but the flange control surfaces; the flange control surface is divided into not mesh, but cross section of circular arc and straight line segments as the deformation prediction and compensation element. The new flange control surfaces are used to replace the original surfaces based on the relationship of geometric elements. So, the form shape model of part with complex flanges in aircraft could be designed rapidly.
2. A CBR-based springback prediction approach is developed to compensate the springback of the bending circular arc segment in one cycle. It is necessary to accumulate enough compensation cases to ensure that springback errors calculated by case base often nearly conform with the practical values. In industrial practice, a great deal of empirical and experimental knowledge is often accessible and increases dynamically, so the developed approach is feasible.

In future, it is necessary to extend the knowledge base to take the compensation factor into consideration for the part with complex structure such as circumferential multiple ladder flanges or radial continuous flanges. The compensation factor is also necessary for cross section curves of different position of the flange boundary line. Additionally, for large size aircraft frame part (more than 1 m long), the forming shape design approach should be developed to control the warp deformation to manufacture industrial parts accurately without manual correction.

Acknowledgements This work is supported by the National Natural Science Foundation of China (Grant No. 51275420 and 51005185).

Compliance with ethical standards

Conflict of interest The authors declare that they have no conflict of interest.

References

1. Antonelli M, Beccari CV, Casciola G, Ciarloni R, Morigi S (2013) Subdivision surfaces integrated in a CAD system. Comput Aided Des 45(11):1294–1305
2. Behrouzi A, Dariani BM, Shakeri M (2009) A one-step analytical approach for springback compensation in channel forming process. Proceedings of the World Congress on Engineering 2009:1757–1762
3. Cafuta G, Mole N, Štok B (2012) An enhanced displacement adjustment method: springback and thinning compensation. Mater Design 40:476–487
4. Cochrane S, Young RI, Case K, Harding J, Gao J, Dani S, Baxter D (2008) Knowledge reuse in manufacturability analysis. Robot Comput-Integr Manuf 24(4):508–513
5. Finnie G, Sun ZH (2013) R^5 model for case-based reasoning. Knowl-Based Syst 16(1):59–65
6. Fu MW, Yong MS, Tong KK, Danno A (2008) Design solution evaluation for metal forming product development. Int J Adv Manuf Technol 38(3):249–257
7. Gan W, Wagoner RH (2004) Die design method for sheet springback. Int J Mech Sci 46(7):1097–1113
8. Guo Y, Peng YH, Hu J (2013) Research on high creative application of case-based reasoning system on engineering design. Comput Ind 64(1):90–103
9. Jamli MR, Ariffin AK, Wahab DA (2014) Integration of feedforward neural network and finite element in the draw-bend springback prediction. Expert Syst Appl 41(8):3662–3670
10. Jiang HJ, Dai HL (2015) A novel model to predict U-bending springback and time-dependent springback for a HSLA steel plate. Int J Adv Manuf Technol 81(5):1055–1066
11. Kappert JH, Houten FJAM, Kals HJJ (1993) Application of features in airframe component design and manufacturing. CIRP Ann-Manuf Technol 42(1):523–526
12. Khan MS, Coenen F, Dixon C, El-Salhi S, Penalva M, Rivero (2015) An intelligent process model: predicting springback in single point incremental forming. Int J Adv Manuf Technol 76(9): 2071–2082
13. Kolesnikov A (2012) Segmentation and multi-model approximation of digital curves. Pattern Recogn Lett 33(9):1171–1179
14. Lingbeek RA, Huétink J, Ohnimus S, Petzoldt M, Weiher J (2005) The development of a finite elements based springback compensation tool for sheet metal products. J Mater Process Technol 169(1): 115–125
15. Lingbeek RA, Meinders T, Ohnimus S, Petzoldt M, Weiher J (2006) Springback compensation: fundamental topics and practical application. In: Proceedings of 9th ESAFORM Conference on Material Forming, pp 403–406
16. Lingbeek RA, Gan W, Wagoner RH, Meinders T, Weiher J (2008) Theoretical verification of the displacement adjustment and springforward algorithms for springback compensation. Int J Mater Form 1(3):159–168
17. Ma Y, Niu WT, Luo ZJ, Yin FW, Huang T (2016) Static and dynamic performance evaluation of a 3-DOF spindle head using CAD–CAE integration methodology. Robot Comput-Integr Manuf 41:1–12
18. Nanu N, Brabie G (2012) Analytical model for prediction of springback parameters in the case of U stretch–bending process as a function of stresses distribution in the sheet thickness. Int J Mech Sci 64(1):11–21
19. Nasrollahi V, Arezoo B (2012) Prediction of springback in sheet metal components with holes on the bending area, using experiments, finite element and neural networks. Mater Design 36(4):331–336
20. Pilani R, Narasimhan K, Maiti SK, Singh UP, Date PP (2000) A hybrid intelligent systems approach for die design in sheet metal forming. Int J Adv Manuf Technol 16(5):370–375
21. Qi J, Hu J, Peng YH (2016) Hybrid weighted mean for CBR adaptation in mechanical design by exploring effective, correlative and adaptative values. Comput Ind 75:58–66
22. Rezayat M (2000) Knowledge-based product development using XML and KCs. Comput Aided Des 32(5):299–309
23. Sheu HT, WC H (1999) Multiprimitive segmentation of planar curves – a two-level breakpoint classification and tuning approach. IEEE Trans Pattern Anal Mach Intell 21:791–797
24. Šormaz D, Arumugam J, Harihara RS, Patel C, Neerukonda N (2010) Integration of product design, process planning, scheduling, and FMS control using XML data representation. Robot Comput-Integr Manuf 26(6):583–595
25. Tadrat J, Boonjing V, Pattaraintakorn P (2012) A new similarity measure in formal concept analysis for case-based reasoning. Expert Syst Appl 39(1):967–972
26. Wang JB, Liu C (2007) Digital sheet metal manufacturing system and application. Proceedings of the ASME International Manufacturing Science and Engineering Conference 2007: 421–428
27. Wang P, Meng P, Zhai JY, Zhu ZQ (2013) A hybrid method using experiment design and grey relational analysis for multiple criteria decision making problems. Knowledge-Based Syst 53:100–107
28. Wang H, Zhou J, Zhao TS, Tao YP (2016) Springback compensation of automotive panel based on three-dimensional scanning and reverse engineering. Int J Adv Manuf Technol 85(5):1187–1193
29. Williams ME, Consolazio GR, Hoit MI (2005) Data storage and extraction in engineering software using XML. Adv Eng Softw 36(11–12):709–719
30. Yang XA, Ruan F (2011) A die design method for springback compensation based on displacement adjustment. Int J Mech Sci 53(5):399–406
31. Zhang ZK, JJ W, Zhang S, Wang MZ, Guo RC, Guo SC (2016) A new iterative method for springback control based on theory analysis and displacement adjustment. Int J Mech Sci 105:330–339